JVI Journals.ASM.org

# Effects of Human Anti-Spike Protein Receptor Binding Domain Antibodies on Severe Acute Respiratory Syndrome Coronavirus Neutralization Escape and Fitness

**Jianhua Sui,[a]* Meagan Deming,[b] Barry Rockx,[b]* Robert C. Liddington,[c] Quan Karen Zhu,[a] Ralph S. Baric,[b] Wayne A. Marasco[a]**

Department of Cancer Immunology and AIDS, Dana-Farber Cancer Institute; Department of Medicine, Harvard Medical School, Boston Massachusetts, USA[a]; Departments of Epidemiology and Microbiology and Immunology, University of North Carolina, Chapel Hill, North Carolina, USA[b]; Infectious and Inflammatory Disease Center, Stanford-Burnham Medical Research Institute, La Jolla, California, USA[c]

## ABSTRACT

**The receptor binding domain (RBD) of the spike (S) glycoprotein of severe acute respiratory syndrome coronavirus (SARS-CoV) is a major target of protective immunity *in vivo*. Although a large number of neutralizing antibodies (nAbs) have been developed, it remains unclear if a single RBD-targeting nAb or two in combination can prevent neutralization escape and, if not, attenuate viral virulence *in vivo*. In this study, we used a large panel of human nAbs against an epitope that overlaps the interface between the RBD and its receptor, angiotensin-converting enzyme 2 (ACE2), to assess their cross-neutralization activities against a panel of human and zoonotic SARS-CoVs and neutralization escape mutants. We also investigated the neutralization escape profiles of these nAbs and evaluated their effects on receptor binding and virus fitness *in vitro* and in mice. We found that some nAbs had great potency and breadth in neutralizing multiple viral strains, including neutralization escape viruses derived from other nAbs; however, no single nAb or combination of two blocked neutralization escape. Interestingly, in mice the neutralization escape mutant viruses showed either attenuation (Urbani background) or increased virulence (GD03 background) consistent with the different binding affinities between their RBDs and the mouse ACE2. We conclude that using either single nAbs or dual nAb combinations to target a SARS-CoV RBD epitope that shows plasticity may have limitations for preventing neutralization escape during *in vivo* immunotherapy. However, RBD-directed nAbs may be useful for providing broad neutralization and prevention of escape variants when combined with other nAbs that target a second conserved epitope with less plasticity and more structural constraint.**

## IMPORTANCE

**The emergence of severe acute respiratory syndrome coronavirus (SARS-CoV) in 2002 and Middle East respiratory syndrome coronavirus (MERS-CoV) in 2012 has resulted in severe human respiratory disease with high death rates. Their zoonotic origins highlight the likelihood of reemergence or further evolution into novel human coronavirus pathogens. Broadly neutralizing antibodies (nAbs) that prevent infection of related viruses represent an important immunostrategy for combating coronavirus infections; however, for this strategy to succeed, it is essential to uncover nAb-mediated escape pathways and to pioneer strategies that prevent escape. Here, we used SARS-CoV as a research model and examined the escape pathways of broad nAbs that target the receptor binding domain (RBD) of the virus. We found that neither single nAbs nor two nAbs in combination blocked escape. Our results suggest that targeting conserved regions with less plasticity and more structural constraint rather than the SARS-CoV RBD-like region(s) should have broader utility for antibody-based immunotherapy.**

Coronaviruses are important human RNA viruses, as exemplified by the global outbreak of the severe acute respiratory syndrome (SARS) coronavirus (SARS-CoV) infection in 2002 to ~2004 and the recently emerged Middle East respiratory syndrome coronavirus (MERS-CoV) in 2012 (1). Both viruses cause severe respiratory tract infection with a high mortality rate (2–5). A wide range of other coronaviruses have also been detected in bats, including SARS-like CoVs, suggesting that they are likely the animal reservoir precursor strains that crossed the species barrier and caused the SARS human epidemic (6–11). Some SARS-like CoVs that are circulating in bats are capable of using human receptors for docking and entry (12) and/or may replicate or recombine with other CoV strains to potentiate cross-species transmission and emerge as new, highly virulent human pathogens (13). Therefore, SARS-CoV and the antigenically distinct SARS-CoV-like bat CoV remain poised for reemergence and represent valuable research models for development of better prevention and treatment strategies against highly heterogeneous zoonotic viruses, including the MERS-CoV. For therapeutic antibody and

Received 31 July 2014 Accepted 14 September 2014

Published ahead of print 17 September 2014

Editor: S. Perlman

Address correspondence to Ralph S. Baric, rbaric@email.unc.edu, or Wayne A. Marasco, wayne_marasco@dfci.harvard.edu.

* Present address: Jianhua Sui, National Institute of Biological Sciences, Beijing, China; Barry Rockx, Departments of Pathology and Microbiology & Immunology, Sealy Center for Vaccine Development, University of Texas Medical Branch, Galveston, Texas, USA.

J.S., R.S.B., and W.A.M. contributed equally to this article and are co-senior authors of the article.



doi:10.1128/JVI.02232-14

vaccine design, it is critically important to develop or elicit broadly cross-reactive neutralizing antibodies (nAbs) that neutralize a broad range of antigenically disparate viruses that share similar pathogenic outcomes *in vivo*. In parallel, it is also essential to uncover nAb-selected virus escape mutation pathways and to pioneer strategies that either prevent escape or drive virus evolution down deleterious pathways that attenuate virus virulence.

The characteristic surface spike (S) protein of SARS-CoV is the major target for vaccines and therapeutic antibodies (14). Numerous SARS S-protein-specific neutralizing antibodies have been reported (15–27). The majority of these nAbs recognize epitopes within the receptor binding domain (RBD) that also bind the angiotensin-converting enzyme 2 (ACE2) receptor (15–18, 21–24, 27, 28). Evidence also suggests that the RBD encodes one of the important neutralizing epitope clusters *in vivo* (29–32). nAbs against S2 were seen during natural human infection with SARS-CoV, but there is a paucity of information on their epitopes and potencies (33). Human nAbs developed as potential therapeutics for the prophylaxis and treatment of SARS mainly targeted the RBD (18, 22–24, 27). Studies have been conducted to assess anti-RBD nAbs for their breadth of protection against all relevant strains of SARS-CoV and neutralization escape variants (34, 35). Some antibodies were broadly active in neutralizing multiple viral strains; however, all nAbs tested, including strain-specific or broadly reactive nAbs, selected for escape mutants. It remains unclear whether there exists an escape-resistant epitope on the RBD or if the RBD is generally not an ideal target for development of escape-resistant broadly neutralizing Abs against the SARS-CoV or any potential novel emerging CoVs.

We previously developed a strain-specific human nAb, 80R, that targets a conformation-sensitive neutralizing epitope located between amino acids (aa) 426 and 492 of the RBD of S glycoprotein (22, 36, 37). 80R is specific against the 2002-2003 SARS-CoV strains, including 2003 early phase (GZ02), middle-phase (CUHK-W1), and late-phase (Urbani and Tor2) epidemic strains (38). It cannot neutralize the 2003-2004 human epidemic strain GD03 or civet (HC/SZ/61/03) or raccoon dog (A031G) 2004 strains due to a single-amino-acid substitution (D480G) in their RBDs, which is also a 80R neutralization escape mutant. To extend the neutralization activity of 80R, a panel of human nAbs (11A, cs5, cs84, fm6, and fm39) were previously developed by *de novo* phage display library selection with GD03-RBD (11A), light-chain shuffling of 80R (cs5 and cs84), or focused mutagenesis of 80R (fm6 and fm39) (38). These 80R derivative nAbs showed broader neutralization activity than parental 80R in viral neutralization assays. Fm6 is the most promising nAb, neutralizing a broad range of viruses, including 2002-2003 strain Tor2, 2003-2004 strain GD03, and 80R's escape mutant (38). In this study, we tested if these nAbs, which convergently target the same or a similar neutralizing epitope within the RBD, alone or in combination can prevent or attenuate viral escape. We first examined if the 80R-derived nAbs with broader neutralizing activity can more effectively neutralize a wide range of natural viral strains as well as 80R's neutralization escape variants that also occurred naturally and next analyzed virological outcome following focused antibody pressure on the neutralization epitope—whether 80R derivatives alone or in combination with 80R can block neutralization escape pathway(s) or force the virus to evolve down an attenuation pathway(s). We showed that some 80R derivative nAbs had great potency and breadth in neutralizing multiple viral strains, including neutralization escape mutant viruses derived from many other nAbs; however, none of them effectively closed escape mutation pathways or significantly attenuated virus pathogenesis *in vivo*. Importantly, a combination of two nAbs against this RBD epitope could also not prevent neutralization escape. We next developed two new RBD-directed nAbs that can neutralize these escape mutant viruses; however, they again selected novel neutralization escape mutants. These results suggest this particular epitope targeted by 80R and its derivatives is structurally flexible and is unlikely to be resistant to neutralization escape *in vivo*. Ideally, to prevent nAb-mediated virus evolution, a more conserved epitope with more sophisticated function and/or structural constraint should be targeted. Alternatively, a divergent combination approach of targeting the RBD-ACE2 interface epitope and a second different epitope may be more effective in providing broad neutralization and prevention of escape variants.

## MATERIALS AND METHODS

**Viruses and cells.** The generation and characterization of each of the recombinant infectious clones (icSARS, icGD03, and icGD03-MA) have been described previously (39, 40). All work was performed in a class II biological safety cabinet in a biosafety level 3 laboratory containing redundant exhaust fans. Personnel were equipped with powered air-purifying respirators with high-efficiency particulate air and organic vapor filters (3M, St. Paul, MN), wore Tyvek suits (DuPont, Research Triangle Park, NC), and were double gloved. Vero E6 cells were grown in minimal essential medium (MEM) (Invitrogen, Carlsbad, CA) supplemented with 10% Fetal clone II (HyClone, South Logan, UT) and gentamicin-kanamycin (UNC Tissue Culture Facility). Viruses were propagated on Vero E6 cells in Eagle's MEM supplemented with 10% Fetal cIone II (HyClone, South Logan, UT) and 1× antibiotic-antimycotic (Gibco, Grand Island, NY) at 37°C in a humidified $CO_2$ incubator; and the virus was cryopreserved at −80°C until use. The viral titers of the stocks were determined on Vero E6 cells by plaque assay as described elsewhere (41, 42).

***In vitro* virus growth.** Cultures of Vero E6 cells were infected with wild-type (WT) or escape mutant viruses at an approximate multiplicity of infection (MOI) of 1 for 1 h, and the monolayer was washed twice with 2 ml of phosphate-buffered saline (PBS) and then overlaid with complete medium. At 3, 8, 12, and 24 h postinfection, supernatant was clarified by centrifugation at 1,600 rpm for 10 min, aliquoted, and frozen at −80°C. Virus stocks were titrated on Vero E6 cells by plaque assay as previously described (41, 42).

**Generation of antibodies by phage display library selection and production of phage Abs and MAbs.** The generation of new antibodies for fm6 escape mutant Urbani Y436H was performed as described previously (38). Phage Abs (in the scFv form [i.e., single-chain antibody variable region]) for individual clones were produced for the pseudotyped virus neutralization assay by the same method for making the phage library (43). Phage particles were concentrated 25× ($2 \times 10^{13}$ to $6 \times 10^{13}$) by using polyethylene glycol (PEG)-NaCl precipitation, dissolved in PBS, and filter sterilized before use. Human monoclonal antibodies (MAbs) (in human IgG1s) were produced as described previously (22). In brief, the $V_H$ and $V_L$ gene fragments of the selected scFvs were separately subcloned into human IgG1 kappa light-chain or lambda light-chain expression vector TCAE5 (44). Human IgG1s were expressed in 293F cells (Invitrogen) or 293T cells by transient transfection and purified by protein A-Sepharose affinity chromatography.

**Neutralization assay with S-protein-pseudotyped lentivirus.** S-protein-pseudotyped lentivirus was produced by cotransfection of 293T cells with four plasmids: S-protein-expressing plasmid, plasmid pCMVΔR8.2 encoding HIV-1 Gag-Pol, and plasmid pHIV-Luc encoding the firefly luciferase reporter gene under the control of the HIV-1 long terminal repeat (LTR), as described elsewhere (37, 38, 45). For the neutralization assay, testing phage-Abs at different dilutions were incubated with an

adequate amount of S-protein-pseudotyped viruses for 30 min at room temperature and then added to a 96-well plate with $1 \times 10^4$ hACE2-expressing 293T cells/well. Thirty-six to 48 h later, infection efficiency was quantified by measuring the luciferase activity in the cell lysate with an EG&G Berthold Microplate luminometer LB 96V.

**Neutralization assay with icSARS-CoV or escape mutants.** Neutralizing titers were determined by either a microneutralization assay or a plaque reduction neutralization titer assay (42). For the microneutralization assay, nAbs were serially diluted 2-fold and incubated with 100 PFU of the different SARS-CoV infectious clone (icSARS-CoV) strains for 1 h at 37°C. The virus and antibodies were then added to a 96-well plate with $5 \times 10^3$ Vero E6 cells/well and 5 wells per antibody dilution. Wells were checked for cytopathic effect (CPE) at 4 to 5 days postinfection, and the 50% neutralization titer was determined as the nAb concentration at which at least 50% of wells showed no CPE. For the plaque reduction neutralization titer assay, nAbs were serially diluted 2-fold and incubated with 100 PFU of the different icSARS-CoV strains for 1 h at 37°C. The virus and antibodies were then added to a 6-well plate with $5 \times 10^5$ Vero E6 cells/well in duplicate. After a 1-h incubation at 37°C, cells were overlaid with 3 ml of 0.8% agarose in medium. Plates were incubated for 2 days at 37°C and then stained with neutral red for 3 h, and plaques were counted. The percentage of plaque reduction was calculated as [1 − (no. of plaques with antibody/no. of plaques without antibody)] × 100. All assays were performed in five replicates.

**Expression and purification of RBD of SARS-CoV mutants and ACE2 proteins for SPR analysis.** Protein expression and purification for surface plasmon resonance (SPR) analysis were performed as follows. Plasmids encoding the RBD (residues 318 to 510) fused C terminally with an Fc tag of human IgG1 were constructed as described elsewhere (46, 47). RBD-Fc fusion proteins were produced by transfection of 293F cells (Invitrogen) and purified by protein A-Sepharose affinity chromatography. Soluble human ACE2 (hACE2) protein corresponding to its N-terminal extracellular domain (aa 18 to 740) (48) was kindly provided by Fang Li at the University of Minnesota Medical School. For mouse ACE2 (mACE2) protein, its N-terminal extracellular domain (aa 19 to 615) was cloned in pcDNA3.1 and fused at the C-terminal portion with a $His_6$-tagged protein, and the protein was produced by transfection of 293F cells and purified by immobilized-metal affinity chromatography (IMAC).

**SPR analysis.** Binding of Abs to different RBDs was analyzed on a Biacore T100 (Biacore) at 25°C, as described previously (38, 49). Anti-human IgG Fc antibody (Biacore) was covalently coated onto a CM5 sensor chip by amine coupling using the coupling kit (Biacore). Abs were captured onto anti-human IgG Fc surfaces at the flow rate of 10 μl/min in HBS buffer (Biacore). ACE2 soluble protein was injected over each flow cell at the flow rate of 30 μl/min in HBS buffer at different concentration ranges, depending on the binding affinity for each Ab. The highest concentration tested for mouse ACE2 reached 20 μM. A buffer injection served as a negative control. Upon completion of each association and dissociation cycle, surfaces were regenerated with 3 M $MgCl_2$ solution. The association rates ($K_a$), dissociation rate constants ($K_d$), and affinity constants ($K_D$) were calculated using Biacore T100 evaluation software. The goodness of each fit was based on the agreement between experimental data and the calculated fits, where the $\chi^2$ values were below 1.0. Surface densities of Abs were optimized to minimize mass transfer. All $K_a$, $K_d$, and $K_D$ values reported here represent the means and standard errors of at least two experiments.

**Escape mutant analysis.** Neutralization-resistant SARS-CoV mutants were generated as described elsewhere (34). In brief, $1 \times 10^6$ PFU of icUrbani, icGD03, or icGD03-MA were preincubated with 30 μg of nAb in 100 μl of medium at 37°C for 1 h and then inoculated onto $10^6$ Vero E6 cells in the presence of the respective Ab at the same concentration. The development of cytopathic effect was monitored over 72 h, and progeny viruses were harvested. nAb treatment was repeated for 2 additional passages, passage 3 viruses were plaque purified in the presence of Ab, and neutralization-resistant viruses were isolated. Experiments were performed in duplicate, and the S glycoprotein gene of individual plaques from each experiment was sequenced as described elsewhere (15). The neutralization titers of wild-type and MAb-resistant viruses were determined as described elsewhere (34, 42).

**Animal studies.** Female BALB/c mice, young (10 weeks old; Jackson Laboratory, Bar Harbor, ME) or aged (12 months old; Harlan Labs, Indianapolis, IN), were acclimated for 1 week after shipping. All mice were housed under sterile conditions in individually ventilated HEPA-filtered Sealsafe cages using the SlimLine system (Tecniplast, Exton, PA). Experimental protocols were reviewed and approved by the Institutional Animal Care and Use Committee at the University of North Carolina, Chapel Hill. For prophylactic passive antibody protection studies, aged mice were injected intraperitoneally with 250 μg of MAb (80R, Fm6, or PBS) in 400 μl PBS 24 h prior to infection. For all viral challenges, mice were anesthetized with a mixture of ketamine (1.3 mg/mouse) and xylazine (0.38 mg/mouse) administered intraperitoneally in a 50-μl volume and then intranasally inoculated with $10^5$ PFU of icUrbani, icGD03, icGD03-MA, fm6 escape mutant (fm6-Esc), fm39-Esc, cs5-Esc, Y12-Esc, or Y112A-Esc. After challenge, morbidity (weight) and mortality were assessed daily. On day 4 postinfection, mice were euthanized with isoflurane, and one-quarter of each mouse lung was taken to determine the viral titer.

**Lung viral titers.** Lung tissue samples were weighed and stored in 1 ml PBS at −80°C until the time of titration. Tissue was thawed and homogenized with glass beads at 60 s at 6,000 rpm in a MagnaLyser (Roche). The solution was centrifuged at 13,000 rpm under aerosol containment in a tabletop centrifuge for 5 min, the clarified supernatant was serially diluted in PBS, and 200-μl volumes of the dilutions were placed onto monolayers of Vero E6 cells in six-well plates. Following 1 h of incubation at 37°C, the cells were overlaid with 0.8% agarose-containing medium. Two days later, the plates were stained with neutral red, and the plaques were counted.

**Statistical analysis.** Statistically significant differences were analyzed by *t* test or analysis of variance (ANOVA) using GraphPad software.

## RESULTS

**Cross-neutralization activities of 80R's derivative human nAbs.** In this study, we tested the neutralization activity of a group of nAbs against a broader panel of wild-type SARS-CoVs and SARS-like-CoVs than that previously tested, including seven available human representative epidemic and zoonotic strains (Fig. 1A). Consistent with previous findings, 11A only neutralized GD03 virus infection. All of the 80R derivatives showed cross-neutralization activity against multiple strains. fm6 demonstrated the greatest cross-strain neutralization activity with effective antibody concentration ranging from 0.02 to 1 μg/ml (Fig. 1B). In addition, 80R and its derivatives were tested against seven additional escape mutant viruses of the 2002-2003 Urbani strain (35), selected by a panel of human nAbs derived from memory B cells of SARS-CoV-infected patients (24). As shown in Fig. 1C, they differentially neutralized all of the mutant viruses tested, with fm6 showing the best overall neutralization potency and breadth. fm6 was further evaluated and compared with 80R for its prophylactic effect in protecting against SARS-CoV challenge in an aged-mouse model. Twelve-month-old BALB/c mice that received fm6 at 12.5 mg/kg intraperitoneally 24 h prior to infection with Urbani or GD03 were protected against significant weight loss. For both the Urbani and GD03 viral challenge groups, all five mice in each fm6-treated group had a more than 3-log reduction in viral titers in their lungs on day 4 after infection to below the assay limit. In contrast, animals that received PBS or 80R were not protected against weight loss or viral load in lungs after challenge with both viruses (Fig. 2). The superiority of fm6 in aged mice demonstrates that it is more potent than 80R and would protect the

A

| | Representative strain name | Amino acid position | | | | | | | |
|---|---|---|---|---|---|---|---|---|---|
| | | 344 | 360 | 442 | 462 | 472 | 479 | 480 | 487 |
| 2002/2003 human outbreak | Tor2/Urbani | K | F | Y | P | L | N | D | T |
| | CUHK-W1 | K | F | Y | P | L | N | D | T |
| | GZ02 | R | F | Y | P | L | N | D | T |
| 2002/2003 Civet | SZ3/SZ16 | R | S | Y | P | L | K | D | S |
| 2003/2004 human outbreak | GD03 | R | S | Y | P | P | N | G | S |
| 2003/2004 Raccoon dog | A031 | R | S | Y | S | P | R | G | S |
| 2003/2004 Civet | HC/SZ/61/03 | R | S | Y | P | P | R | G | S |

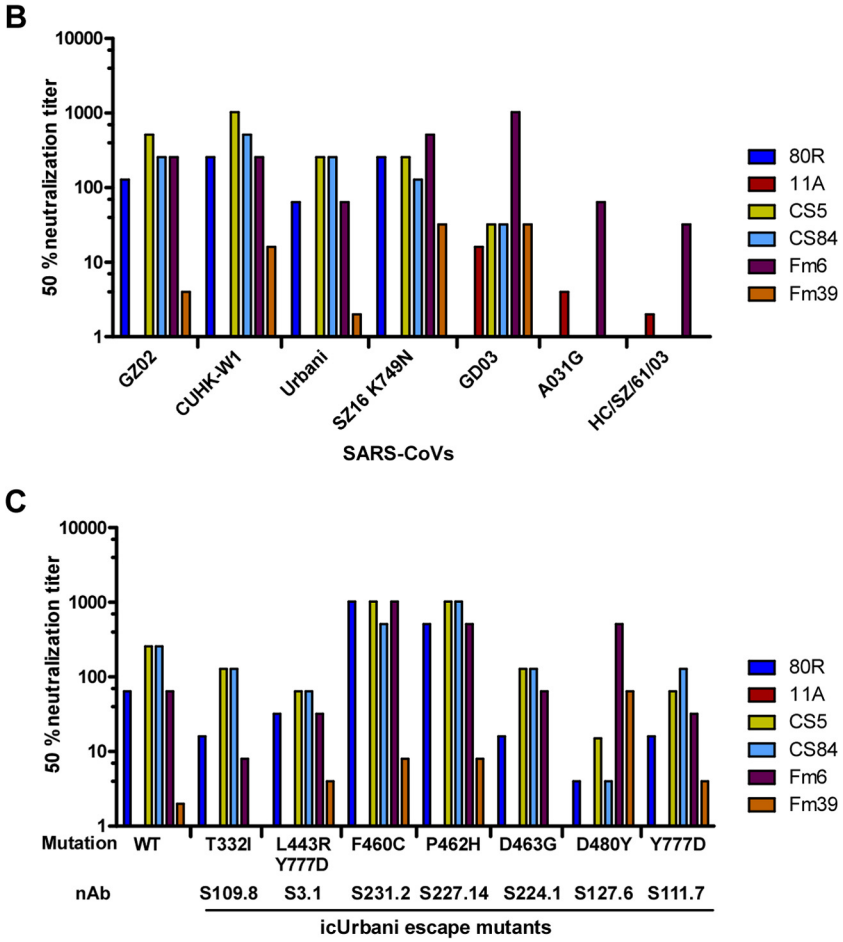


**FIG 1** Neutralization of human and animal SARS-CoVs and neutralization escape mutants by a panel of nAbs. (A) Amino-acid differences in the RBDs of human and animal SARS-CoVs. (B) Neutralization of viruses listed in panel A by 80R, its derivative antibodies, and 11A (GD03 specific and not a derivative of 80R) in a microneutralization assay. The 50% neutralization titer was defined as the Ab dilution at which at least 50% of wells showed no CPE. The Ab concentration in the stock solution used for dilution was 20 μg/ml. (C) Neutralization efficacy against wild-type (WT) and neutralization escape mutants generated in a previously reported study (34) by the same panel of nAbs tested in panel B. The neutralization assay was performed similarly to that in panel B.

most vulnerable aged populations from life-threatening disease. 80R has been previously shown to significantly reduce virus titers in lungs of young mice that were infected with Urbani virus (37). SARS-CoV is more virulent in aged than in young mice, as evidenced by increased virus titers, more severe disease outcomes, and higher mortality rates in aged populations, similarly to what has been reported for humans (50). This increased virulence may be responsible for the different effects of 80R seen in aged and young mice. On the other hand, the lung titer was examined on day 2 post-viral infection in the previously published study (37), whereas it was examined on day 4 postinfection in this study. We therefore cannot rule out

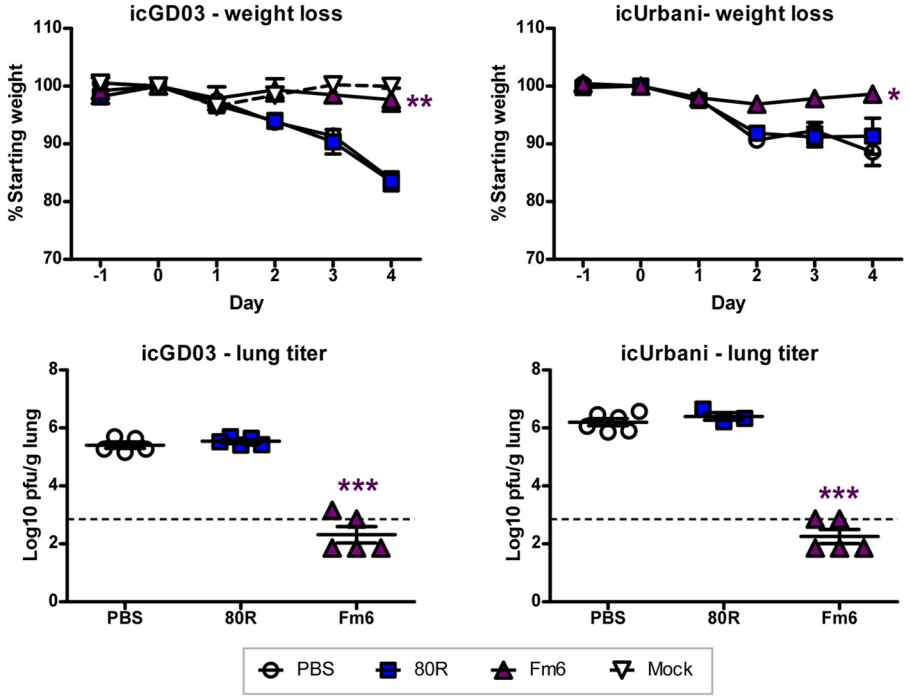


**FIG 2** Prophylactic treatment of SARS-CoV infections in 12-month-old BALB/c mice by 80R and fm6 nAbs. Body weights of mice infected with icGD03 or icUrbani were measured daily after passive administration of 12.5 mg/kg (~250 μg/mouse) nAbs. Lung tissues of mice infected with icGD03 or icUrbani were harvested on day 4 postinfection and assayed for infectious virus by a plaque assay using Vero E6 cells. Error bars indicate standard deviations ($n = 5$). *, $P < 0.01$, **, $P < 0.001$, and ***, $P < 0.0001$, compared with the PBS group.

the possibility that an 80R escape mutant virus may have rapidly emerged during this 2-day window, which may also account for the inability of 80R to protect aged mice from infection.

**Neutralization escape mutants from 80R derivatives.** To test if SARS-CoV could escape from neutralization by the 80R derivatives, *in vitro* neutralization escape studies were performed with the Urbani isolate under the selection of 80R and its derivatives, cs5, cs84, fm6, and fm39, which have the amino acid differences in light-chain complementarity-determining regions (LCDRs) (38). Escape mutants were isolated from all nAbs, and all mutants contained single-amino-acid changes within the RBD (Fig. 3A). Consistent with our previous report, the 80R escape mutants had aspartic acid-to-glycine or -alanine (D480G or D480A) substitutions (38). Two neutralization escape isolates of cs5 had amino acid changes at two different sites: one had an N479I mutation, and the other had a D480Y mutation. The single-amino-acid changes associated with neutralization escape from cs84, fm6, and fm39 were D480Y, Y436H, and N479T, respectively. Of note, 80R escape mutant Urbani-D480G virus was no longer able to escape the neutralization of fm6: no mutant was generated in three independent experiments (data not shown), indicating that once the virus undergoes its primary escape (D480G under the selection of 80R), further evolution is heavily restricted and limits the virus's ability to evolve secondary escape mutations across this region (e.g.Y436H or another pathway).

**Generation of new nAbs Y12 and Y112A to neutralize fm6's escape mutant Y436H.** As shown in Fig. 3B, fm6 can cross-neutralize all of the escape mutant viruses, except for the N479T mutant selected by fm39, and thus represents the most broadly neutralizing and potent nAb in the panel. Despite its broad neutralization potency, the occurrence of the Y436H escape mutant following selection with fm6 led us to identify new nAbs that could have even broader activity, including blockade of the Y436H escape pathway. We took a similar approach to that used before (38) for generating nAbs against the Y436H mutant. Purified RBD (aa 318 to 510) of Tor2 (a strain identical to Urbani across the RBD) containing the Y436H mutant was prepared for Ab-phage library panning. Two combined nonimmune human antibody-phage display libraries and a light-chain-shuffled 80R-vk-cs library (38) were panned against the Y436H-RBD protein either coated on immunotubes or covalently coupled to magnetic beads, separately. Using a neutralization assay with Tor-Y436H-pseudotyped virus, two nAbs (Y12 and 22) were identified from the nonimmune antibody libraries, and eight nAbs (55, 61, 95, 100, 109, Y112A, 113, and 132) were isolated from the 80R-vk-cs library. Sequence comparison of these antibodies is shown in Fig. 3C. These 10 antibodies were further analyzed for cross-neutralization activity against four more pseudotyped viruses. As shown in Fig. 3D, 2 of the 10 antibodies, Y12 and Y112A, efficiently neutralized all strains tested, including human strains (Tor2 and GD03) and those containing the 80R (D480A or D480G) and the Fm6 (Y436H) escape mutations. Plaque reduction assay confirmed the broad neutralization activities of Y12 and Y112A against wild-type human strains Urbani and GD03, 80R neutralization-escape mutant virus (Urbani-D480G), and fm6 escape mutant (Urbani-Y436H) as well as a mouse-adapted strain, GD03-MA virus, which carries the GD03 S glycoprotein with a Y436H mutation in the RBD (Fig. 4). Y112A and Y12 similarly neutralized Urbani-

A

| Ab | Ab sequence difference | | | Virus under selection | Escape mutant |
|---|---|---|---|---|---|
| | LCDR1-aa161-164 | LCDR2-aa182-186 | LCDR3-aa223-225 | | |
| 80R | VRSN | DASTR | RSN | Urbani | D480G or D480A |
| Cs5 | INNN | DASTR | RSN | Urbani | D480Y or N479I |
| Cs84 | VNNN | DASTR | RSN | Urbani | D480Y |
| Fm6 | TENN | DASTR | RSN | Urbani | Y436H |
| | | | | Urbani-D480G | None |
| Fm39 | AENN | DASTR | RSN | Urbani | N479T |

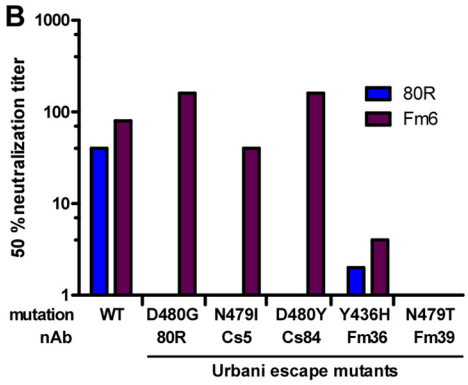


C

| Ab clone # | LCDR1 aa161-164 | LCDR2 aa182-186 | LCDR3 aa223-225 |
|---|---|---|---|
| 80R | VRSN | DASTR | RSN |
| fm6 | TEN. | .... | ... |
| Y112A | .NN. | | .F. |
| 55 | .S.. | G..N. | .Y. |
| 61 | .S.. | G..I. | ... |
| 95 | IRS. | | .F. |
| 100 | INN. | | .FI |
| 109 | INN. | | .F. |
| 113 | .S.. | | .F. |
| 132 | .SN. | | .Y. |
| Y12 or 22 | Totally different VH and VL | | |

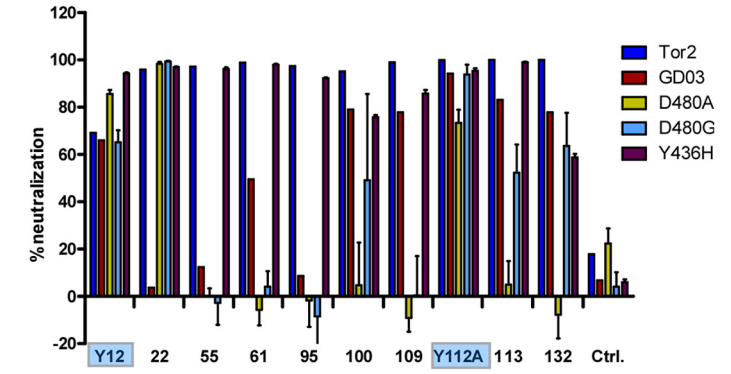


**FIG 3** Neutralization escape mutants of 80R derivatives and generation of new antibodies to neutralize escape mutants. (A) Sequence comparison of 80R derivative nAbs in their light-chain complementarity-determining regions (LCDR1 to -3) (38) and their escape mutations in the RBD. (B) Cross-neutralization of escape mutant viruses listed in panel A by fm6. The neutralization assay was performed similarly to that in Fig. 1. 80R was included as a control. (C) Sequence comparison of human monoclonal Abs against the fm6 escape mutant Urbani-Y436H in their LCDRs. A dot indicates the same residue as that of 80R. These Abs were isolated from selection of nonimmune phage display antibody library (Abs 12 and 22) and 80R-cs Ab-phage display libraries (all other Abs) (38) using Tor2-Y436H-S1 protein coupled onto magnetic beads or the immunotube as the panning targets. (D) Neutralization of S protein of SARS-CoV-pseudotyped lentiviruses with antibodies listed in panel C. Ab Y12 and Y112A (highlighted in blue) have broadly neutralization activity against all five viruses tested.

Y436H, but Y112A was more potent in neutralizing the Urbani, GD03, and Urbani-D480G viruses.

**Neutralization escape mutants of Y12, Y112A, and the combination of 80R and fm6.** We next examined the escape profiles from Y12 and Y112A of a number of viral strains, including escape mutants of 80R and fm6. As shown in Fig. 5A, some of the mutants were previously seen following selection with other 80R derivative antibodies. As fm6, Y12, and Y112A alone failed to prevent viral escape mutations, we next asked if a convergent combination immunotherapy (CCI) approach, in which two nAbs that are directed against the same or a similar epitope, can prevent neutralization escape or seriously impact viral fitness. The observation that the icUrbani-D480G mutant virus selected by 80R was no longer able to escape the neutralization of fm6 indicates that the virus could only undergo one round of mutation when the viruses were sequentially targeted by 80R and then fm6. We therefore tested if the same evolutionary limitations exist when both of them are combined and used simultaneously. The result showed that the combination did not prevent the emergence of viral escape mutants: rather, a resistant virus carrying the N479T mutation was selected (Fig. 5A). Urbani-N479T is also an escape mutant of nAb fm39, which neither 80R nor fm6 alone neutralized (Fig. 3A and B). Taken together, 80R and all of its derivatives are selecting for slightly variant escape profiles across the 80R epitope. These escape mutations occur at 5 positions along the interface between 80R and the RBD, which are either directly adjacent to or the key contact residues for binding with hACE2 in the RBD (Fig. 5B).

**Effect of escape mutations on human ACE2 receptor binding and *in vitro* viral growth.** In order to test if the escape mutants generated from the above studies alter virus entry and fitness, we determined binding affinity and kinetics between the RBDs of these escape mutants and soluble extracellular domain of human ACE2 (hACE2). Although most of the mutations occurred at positions at the RBD-hACE2 interface (48), they did not appreciably change the binding affinity ($K_D$) and kinetics ($K_{on}$ and $K_{off}$) to hACE2, except Y12's escape mutation (Y442S), which had an ~6-fold-slower $K_{off}$ and an ~5-fold-increased affinity (Fig. 5C). Replication of all viruses in Vero E6 cells (expressing monkey ACE2) was delayed early in infection, as shown by a 1- to 2-log reduction in titer at 8 h after infection compared with wild-type icUrbani. However, all viruses reached comparable peak titers of between $10^6$ and $10^7$ PFU/ml by 24 h after infection (Fig. 5D). The monkey ACE2 of Vero E6 (GenBank accession no. AY996037.1)

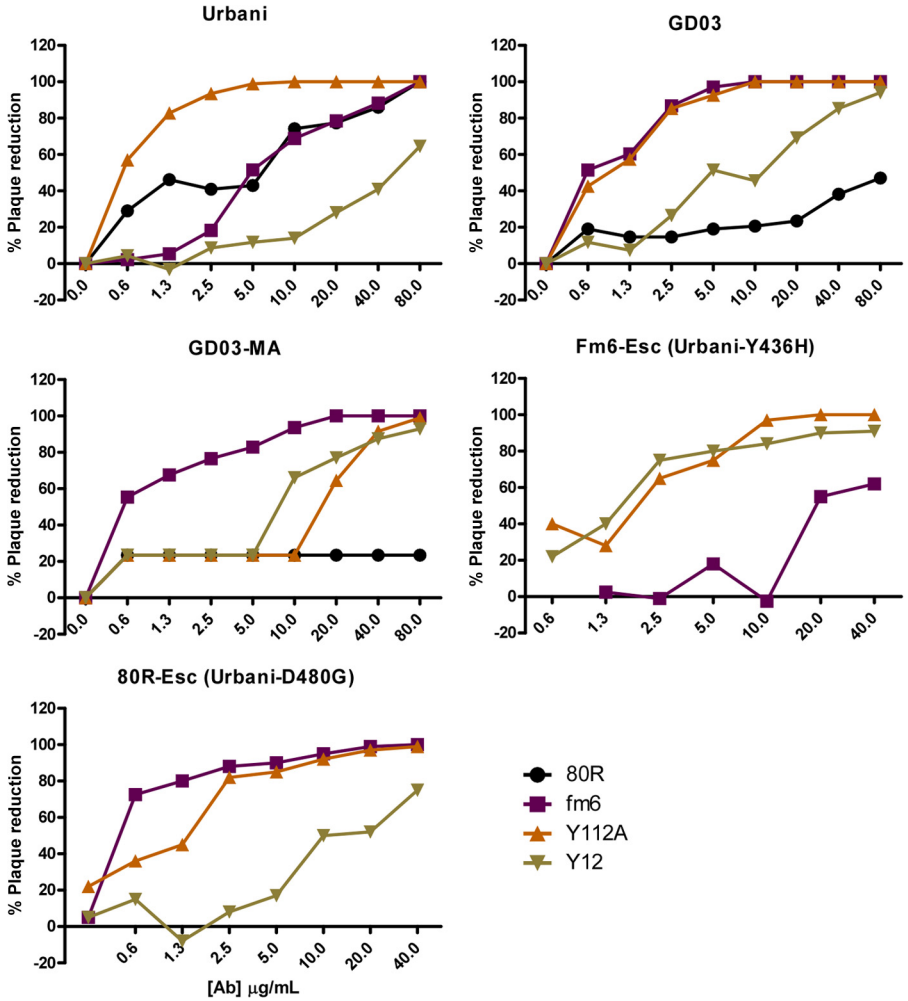


**FIG 4** Broadly neutralizating activity of nAbs fm6 and Y112A. Neutralization titers against five different SARS-CoVs or escape mutants were determined in a plaque reduction neutralization assay. Abs were serially diluted 2-fold as indicated, and 100 PFU of the different icSARS-CoV strains was used (see Materials and Methods). At the end of the assay, plaques were stained and counted for calculation of plaque reduction efficiency. Each value shown represents the average of duplicate samples. GD03-MA is a mouse-adapted strain encoding the 2004 human GD03 S protein with Y436H mutation in the RBD (39).

has 94.5% amino acid sequence identity to hACE2, and they have identical sequences among the 18 amino acids that make contact with SARS-CoV RBD (48). Thus, the viral replication kinetics in Vero E6 likely represents that which occurs in human host cells. The results show that the escape mutants grow with delayed kinetics but with equal peak titers in Vero E6 cells *in vitro*, indicating a likely similar viral replication pattern in human hACE2-expressing host cells.

**Effect of escape mutations within the Urbani background on *in vivo* virus growth.** *In vivo* pathogenesis study of some of these escape mutants in 12-month-old mice showed that cs5-N479I and fm39-N479T mutant viruses were attenuated. Mice infected with these two viruses showed significantly less weight loss (less than 5%) than those infected with wild-type Urbani virus (Fig. 5E). In addition, cs5-N479I mutant virus had a significant reduction in viral titer in the lungs. It is known that infection of murine cells with SARS-CoVs is inefficient, primarily due to very weak binding between RBDs and mACE2 (51). Indeed, by Biacore analysis, we found that the binding affinity of the wild-type Urbani virus RBD to mACE2 was very low (estimated to be lower than 20 μM, hundreds of folds less than that to hACE2), while the kinetics and affinities of all other mutants were not measureable (data not shown). These data are consistent with the possibility that the N479I and N479T mutations resulted in a further loss of binding affinity to mACE2.

**Effect of escape mutations within GD03 background on *in vivo* virus growth in a mouse model.** A series of neutralization escape mutants of Y12 and Y112A were also generated on the background of GD03 and GD03-Y436H viruses (Fig. 6A), the latter containing the same Y436H mutation in the RBD as the highly pathogenic MA15 strain (52), which is a mouse-adapted lethal SARS-CoV in young mice. Two escape mutations of GD03 virus, P462L and N479I, selected by Y12 and Y112A, respectively, had minimal effect on kinetics or binding affinity to hACE2. In contrast, two escape mutations from GD03-Y436H virus, Y442L and S487T, selected by Y12 and Y112A, respectively, increased the binding affinity to hACE2 about 4-fold compared with GD03-Y436H or wild-type GD03. Both the GD03-Y436H Y442L and GD03-Y436H S487T mutant viruses showed increased *in vivo* growth in young mice, with a more than 2-log increase in viral titer

A

| Position in RBD | Ab | Mutation | Virus under selection |
|---|---|---|---|
| 436 | fm6 | Y436H | Urbani-WT |
| | Y112A | Y436R | Urbani-Y436H (Fm6-Esc) |
| 442 | Y12 | Y442S | Urbani-WT |
| 479 | cs5 | N479I | Urbani-WT |
| | fm39 | N479T | Urbani-WT |
| | 80R+fm6 | N479T | Urbani-WT |
| 480 | 80R | D480A or D480G | Urbani-WT |
| | cs5 | D480Y | Urbani-WT |
| | Y112A | D480A | Urbani-WT |
| | Y112A | D480G | Urbani-Y436H (Fm6-Esc) |
| | Y112A | D480V | Urbani-D480G (80R-Esc) |
| 485 | Y112A | T485A | Urbani-D480G (80R-Esc) |

B

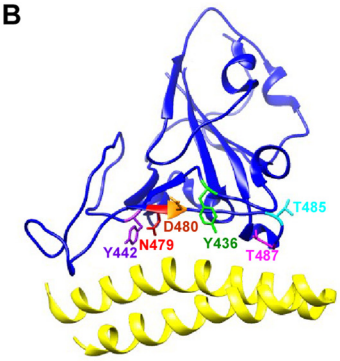


C

| Ab | Virus under selection | RBD binding with hACE2 | | | |
|---|---|---|---|---|---|
| | | | Ka ($M^{-1}s^{-1}$ x $10^5$) | Kd ($s^{-1}x10^{-2}$) | KD (nM) |
| No Ab | Urbani-WT | WT | 6.2±0.9 | 4.0±0.1 | 65.0±10.9 |
| 80R | Urbani-WT | D480G | 5.4±1.1 | 7.4±4.1 | 139±21.5 |
| CS84 or CS5 | Urbani-WT | D480Y | 5.7±0.8 | 3.4±0.0 | 60.0±10.2 |
| 80R or Y112A | Urbani-WT | D480A | 4.7±0.3 | 3.8±0.3 | 81.0±0.5 |
| Y12 | Urbani-WT | Y442S | 5.0±0.0 | 0.7±0.0 | 13.0±0.0 |
| Fm6 | Urbani-WT | Y436H | 5.0±0.0 | 3.6±0.0 | 71.0±0.1 |
| CS5 | Urbani-WT | N479I | 4.1±0.3 | 1.9±0.0 | 46.3±0.3 |
| Fm6+80R or fm39 | Urbani-WT | N479T | 5.5±2.4 | 3.7±1.5 | 67.5±0.3 |
| Y112A | Urbani-Y436H | Y436H /D480G | 4.0±0.1 | 4.6±0.0 | 113.0±4.6 |

D

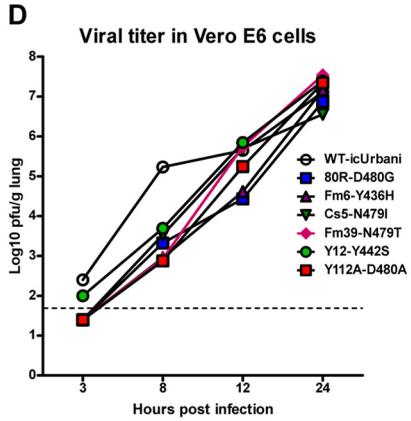


E

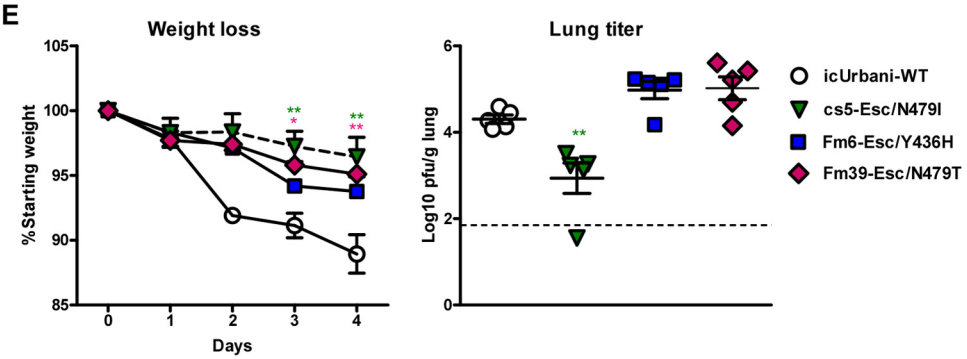


**FIG 5** Effects of escape mutations within the Urbani background on the binding to ACE2 and viral growth i*n vitro* and *in vivo*. (A) List of all critical amino acid changes associated with escape mutation. (B) The locations of the amino acids listed in panel A are shown in the cocrystal structure of the SARS-CoV RBD (blue) and its receptor, human ACE2 (yellow) (PDB code 2AJF). (C) Binding affinity and kinetics measurement of the RBD of the escape mutations listed in panel A to human ACE2. Binding kinetics were evaluated using a 1:1 Langmuir binding model. Each $K_a$, $K_d$, and $K_D$ value represents the mean and standard error of two independent experiments run on Biacore. (D) *In vitro* growth characteristics of neutralization escape mutant SARS-CoV. Cultures of Vero E6 cells were infected in duplicate with icUrbani WT and neutralization escape mutants as indicated at a multiplicity of infection (MOI) of 1, as described in Materials and Methods. Virus titers at different time points were determined by a plaque assay using Vero E6 cells. A dotted line indicates the lowest detectable virus titer. (E) Escape mutants of cs5, cs39, and fm6 in aged mice (12 months old). (Left) Weight loss. All mice were inoculated with $10^5$ PFU of viruses as indicated. Body weights of infected mice were measured on a daily basis (5 mice per group). Weight changes are expressed as the mean percent changes for infected animals relative to the initial weights at day 0. *, $P < 0.05$, and **, $P < 0.01$, compared with the icUrbani WT, by two-way analysis of variance. (Right) Lung titers. Lung tissues were harvested from infected mice on day 4 after infection and were assayed for virus titer by a plaque assay using Vero E6 cells. A dotted line indicates the lowest detectable virus titer.

in the lungs by day 4 after infection, compared with GD03-Y436H (Fig. 6B). In addition, mice infected with these two mutants showed more body weight loss: in particular, mice infected with the Y12 escape mutant lost up to 15% of their weight by day 4 after infection, significantly higher than mice infected with GD03-Y436H (Fig. 6B). In agreement with the greater *in vivo* weight loss of the Y12-Y442L escape mutant, its binding affinity to mouse ACE2 was weak ($K_D$, ~400 nM), making it the only RBD with measurable affinity to mouse ACE2 among the many others tested under the same conditions (Fig. 6A).

## DISCUSSION

The RBDs of coronaviruses typically vary in length and sequence, consistent with their structural and functional flexibility in bind-

A

| Ab | Virus under selection | RBD binding with hACE2 | | | |
|---|---|---|---|---|---|
| | | Mutation | Ka ($M^{-1}s^{-1}$ x $10^5$) | Kd ($s^{-1}$x$10^{-2}$) | KD (nM) |
| No Ab | GD03-WT | WT | 8.9±0.8 | 35.8±8.2 | 401±58.5 |
| | GD03-Y436H | Y436H | 7.1±0.0 | 15.2±0.0 | 425±23.3 |
| Y12 | GD03 | P462L | 6.0±0.3 | 24.3±0.2 | 409±18.2 |
| Y12 | GD03-Y436H | Y436H/Y442L | 5.8±0.4 | 6.2±0.5 | 107±0.6 |
| Y112A | GD03 | N479I | 5.0±0.3 | 19.2±0.2 | 365±19.0 |
| Y112A | GD03-Y436H | Y436H/S487T | 5.1±0.2 | 5.2±0.2 | 102±0.2 |
| Y12 | GD03-Y436H | | RBD binding with mACE2 | | |
| | | Y436H/Y442L | 9.3 | 36.6 | 392 |

B

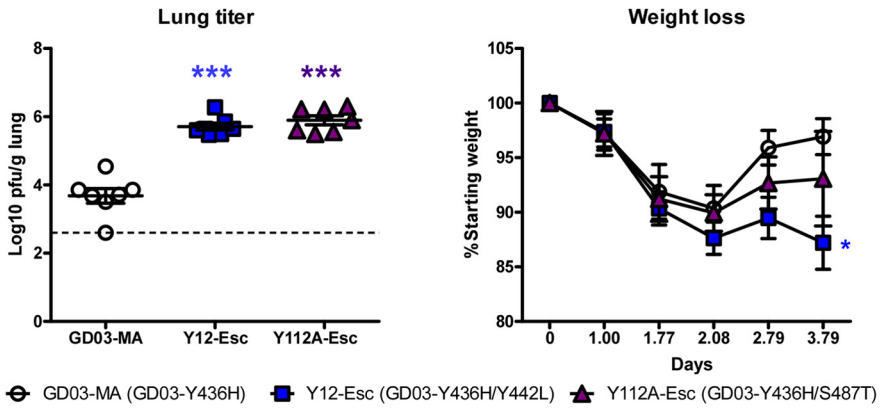


**FIG 6** Effect of escape mutations within the GD03 background on the binding to ACE2 and *in vivo* virus growth in mouse model. (A) A table lists escape mutants generated with icGD03 or icGD03-MA (Y436H) viruses for nAb Y12 and Y112A and the binding kinetics of the RBD of these escape mutants with human ACE2 and mouse ACE2 (mACE2). (B) Escape mutants of Y12 and Y112A in young mice (10 weeks old). The experiment was performed similarly to that in Fig. 5E. (Left) Virus titer in lungs. Lung tissues were harvested from infected mice on day 4 after infection for virus titer analysis. Error bars denote standard deviations. *, $P < 0.05$, and ***, $P < 0.0001$, compared with the GD03-MA strain. A dotted line indicates the lowest detectable virus titer. (Right) Weight loss. Body weights of infected mice were monitored at different time points (5 mice per group). Weight changes are expressed as the mean percent changes for infected animals relative to the initial weights at day 0.

ing to different receptors. In this study, with a large panel of nAbs against the RBD of SARS-CoVs, we aimed to test if the RBD is a susceptible region to escape mutations in general, whether a single- or double-RBD-targeting nAb can prevent escape mutations, and if not, whether the escape mutants are attenuated or more virulent. We first examined the nAbs we previously identified for their cross-neutralization activities against a full panel of human and animal SARS-CoV isolates and escape mutants of other RBD-targeting nAbs. We found that fm6 is the most potent nAb with the broadest neutralization activity *in vitro* (Fig. 1, 3, and 4) and protected 12-month-old mice from infection by the virulent epidemic SARS-CoV human strain Urbani and the less virulent human strain GD03 (Fig. 2). However, a neutralization escape mutation, Y436H, developed when the Urbani virus was placed under the selection of fm6. Two new nAbs, Y12 and Y112A, were developed against the Y436H mutant. Both of these nAbs also showed broadly neutralizing activities to other viral strains (Fig. 3C and D and Fig. 4); however, they did not block the emergence of new escape mutants to these nAbs. Detailed analysis of all of the nAb escape mutants of strain Urbani showed that they selected for slightly variant escape profiles along the interface between ACE2 and the RBD (Fig. 5A and B). Although these mutations are at positions either adjacent to or including the key contact residues for binding to the hACE2 receptor, most did not appreciably affect binding. The exception, Y442S, resulted in an increased binding affinity. In addition, these mutations affected virus growth *in vitro* in monkey ACE2-expressing Vero E6 cells at 8 h postinfection, but peak titers were not significantly different from those of the wild-type icUrbani strain (Fig. 5D).

Neutralization escape mutations can result in attenuation or increased virulence. Neutralization mutants for nAb cs5 and fm39, Urbani-N479I and Urbani-N479T, respectively, showed significant attenuation in 12-month-old mice. The fm6 neutralization escape mutation, Y436H, is associated with the adaptation of a mouse adapted MA15 virus (52). Of the six mutations of the MA15 genome that confer lethality in young mice, only the Y436H mutation is in the S protein. However, the fm6 escape mutant, Urbani-Y436H, showed no adaptation benefit but rather a slight attenuation in aged mice, which is in agreement with a recent report that the Y436H mutation is necessary but not sufficient in contributing to the adaptation (50). Although structural modeling suggests that the Y436H change may increase binding with D38 of mouse ACE2 via electrostatic interaction (50), this was not confirmed in our Biacore studies. The binding of RBDs of the wild type and the escape mutants with mouse ACE2 was very weak ($K_D$, >20 μM), except for the escape mutant that contains a double mutation of Y436H and Y442L in the RBD of GD03 virus. This double mutation dramatically increased the binding affinity of RBD to mouse ACE2, reaching 400 nM, which is the only mutant with measurable binding affinity to mACE2 by Biacore. Indeed, 10-week-old mice infected with this mutant virus exhibited up to 15% weight loss, demonstrating that this mutant is significantly

more virulent than GD03-MA virus, which contains a single Y436H mutation in the RBD of GD03 (Fig. 6B). Importantly, the Y442L change has also been reported to be associated with increased virulence of a mouse-adapted MA20 virus on the background of Urbani (50). These results support that the Y442L change mediates higher-affinity mouse ACE2 binding and likely contributes to the increased virulence in mice. For binding to human ACE2, this Y442L change and the S487T mutation in the same background virus (GD03-Y436H) also increased binding affinity ~4-fold compared with that of the wild-type GD03 or GD03-Y436H background strain. The S487T mutation has been previously noted to be important for adaption of SARS-CoV from civets to humans (53).

80R and all of its derivative nAbs selected for slightly variant escape mutants along the interface of ACE2 and RBD, confirming that they all recognize a very similar epitope. These nAbs provided a unique tool set to test if a convergent combination immunotherapy (CCI) approach in which two or more nAbs that are directed against the same or a similar epitope can prevent neutralization escape or attenuate the escaping virus. With two nAbs (80R and fm6), different results were obtained, depending on if they were used sequentially or simultaneously. When 80R was used first, and after its escape mutant Urbani-D480G was developed, no further escape mutant could be selected following fm6 neutralization. However, the same evolutionary constraint did not exist when both nAbs were used simultaneously; the virus took a new escape pathway (N479T, a mutation that did not change hACE2 binding) to escape the neutralization of 80R and fm6. Although this result suggests that CCI against this particular RBD epitope may be possible, it may not be optimal for treating SARS-CoV. Rani et al. (54) reported an 80R-derived antibody with a 270-fold-increased affinity, SK4, that showed greater neutralization potency as well as reduced susceptibility to escape mutations; however, it remains to be tested if RBD-directed nAbs with superior affinity could improve the CCI strategy.

On the other hand, a divergent combination immunotherapy (DCI) approach of using a combination of nAbs targeting different neutralizing epitopes is likely to be superior over CCI to provide broader protection and reduce or eliminate the possibility of generating escape variants. Fm6 cross-neutralized escape mutant viruses generated for other broadly nAbs (Fig. 1B), including the T332I mutant of nAb S109.8. This nAb recognizes an epitope in the RBD that is distinct from fm6 and does not interfere with the binding with ACE receptor (35). Thus, fm6 may be a good candidate for divergent combination with S109.8 in preventing escape and providing neutralization against a broader range of viruses. In addition and in contrast to the N-terminal RBD, the C-terminal S2 domain of spike protein is highly conserved and contains the functional elements required for membrane fusion, which usually places strong evolutionary constraints on the sequence (55). It has been demonstrated that nAbs targeting the conserved stem region of the hemagglutinin (HA) of influenza A and B viruses possess broad neutralizing activity and are highly resistant to neutralization escape compared to nAbs that target the highly variable HA's globular head, which is responsible for sialic acid receptor binding (56). Similarly, the S2 domain of SARS-CoV may be an ideal target for developing nAbs with greater breadth, potency of neutralization, and resistance to neutralization escape. Such S2-directed nAbs can be used alone or as part of a DCI approach.

In summary, our results show that using either single nAbs or dual nAb combinations to target a SARS-CoV RBD epitope that shows plasticity may have limitations for preventing nAb-mediated evolution during *in vivo* immunotherapy. However, RBD-directed nAbs may be particularly useful for providing broad neutralization and prevention of escape variants when combined with other nAbs that target a second conserved epitope with less plasticity and more structural constraint. In addition, our iterative approach to broaden the activity of a nAb based on its neutralization escape profile remains valid as a strategy to enhance their breadth and potency and as part of an investigation to prioritize the targetable epitopes that are not all equal in their ability to undergo neutralization escape. The recently emerged MERS-CoV provides a timely opportunity to apply these principles.

## ACKNOWLEDGMENT

This work was supported by NIH U01-AI061318 and R01AI085524 to W.A.M.

## REFERENCES

1. **Zaki AM, van Boheemen S, Bestebroer TM, Osterhaus AD, Fouchier RA.** 2012. Isolation of a novel coronavirus from a man with pneumonia in Saudi Arabia. N. Engl. J. Med. **367:**1814–1820. http://dx.doi.org/10.1056/NEJMoa1211721.
2. **Ksiazek TG, Erdman D, Goldsmith CS, Zaki SR, Peret T, Emery S, Tong S, Urbani C, Comer JA, Lim W, Rollin PE, Dowell SF, Ling AE, Humphrey CD, Shieh WJ, Guarner J, Paddock CD, Rota P, Fields B, DeRisi J, Yang JY, Cox N, Hughes JM, LeDuc JW, Bellini WJ, Anderson LJ.** 2003. A novel coronavirus associated with severe acute respiratory syndrome. N. Engl. J. Med. **348:**1953–1966. http://dx.doi.org/10.1056/NEJMoa030781.
3. **Liang G, Chen Q, Xu J, Liu Y, Lim W, Peiris JS, Anderson LJ, Ruan L, Li H, Kan B, Di B, Cheng P, Chan KH, Erdman DD, Gu S, Yan X, Liang W, Zhou D, Haynes L, Duan S, Zhang X, Zheng H, Gao Y, Tong S, Li D, Fang L, Qin P, Xu W.** 2004. Laboratory diagnosis of four recent sporadic cases of community-acquired SARS, Guangdong Province, China. Emerg. Infect. Dis. **10:**1774–1781. http://dx.doi.org/10.3201/eid1010.040445.
4. **Marra MA, Jones SJ, Astell CR, Holt RA, Brooks-Wilson A, Butterfield YS, Khattra J, Asano JK, Barber SA, Chan SY, Cloutier A, Coughlin SM, Freeman D, Girn N, Griffith OL, Leach SR, Mayo M, McDonald H, Montgomery SB, Pandoh PK, Petrescu AS, Robertson AG, Schein JE, Siddiqui A, Smailus DE, Stott JM, Yang GS, Plummer F, Andonov A, Artsob H, Bastien N, Bernard K, Booth TF, Bowness D, Czub M, Drebot M, Fernando L, Flick R, Garbutt M, Gray M, Grolla A, Jones S, Feldmann H, Meyers A, Kabani A, Li Y, Normand S, Stroher U, Tipples GA, Tyler S, Vogrig R, Ward D, Watson B, Brunham RC, Krajden M, Petric M, Skowronski DM, Upton C, Roper RL.** 2003. The genome sequence of the SARS-associated coronavirus. Science **300:**1399–1404. http://dx.doi.org/10.1126/science.1085953.
5. **Rota PA, Oberste MS, Monroe SS, Nix WA, Campagnoli R, Icenogle JP, Penaranda S, Bankamp B, Maher K, Chen MH, Tong S, Tamin A, Lowe L, Frace M, DeRisi JL, Chen Q, Wang D, Erdman DD, Peret TCT, Burns C, Ksiazek TG, Rollin PE, Sanchez A, Liffick S, Holloway B, Limor J, McCaustland K, Olsen-Rasmussen M, Fouchier R, Gunther S, Osterhaus ADME, Drosten C, Pallansch MA, Anderson LJ, Bellini WJ.** 2003. Characterization of a novel coronavirus associated with severe acute respiratory syndrome. Science **300:**1394–1399. http://dx.doi.org/10.1126/science.1085952.
6. **Anderson LJ, Tong S.** 2010. Update on SARS research and other possibly zoonotic coronaviruses. Int. J. Antimicrob. Agents **36**(Suppl 1):S21–S25. http://dx.doi.org/10.1016/j.ijantimicag.2010.06.016.
7. **Hon CC, Lam TY, Shi ZL, Drummond AJ, Yip CW, Zeng F, Lam PY, Leung FC.** 2008. Evidence of the recombinant origin of a bat severe acute respiratory syndrome (SARS)-like coronavirus and its implications on the direct ancestor of SARS coronavirus. J. Virol. **82:**1819–1826. http://dx.doi.org/10.1128/JVI.01926-07.
8. **Lau SK, Woo PC, Li KS, Huang Y, Tsoi HW, Wong BH, Wong SS, Leung SY, Chan KH, Yuen KY.** 2005. Severe acute respiratory syndrome coronavirus-like virus in Chinese horseshoe bats. Proc. Natl. Acad. Sci. U. S. A. **102:**14040–14045. http://dx.doi.org/10.1073/pnas.0506735102.

9. **Li W, Shi Z, Yu M, Ren W, Smith C, Epstein JH, Wang H, Crameri G, Hu Z, Zhang H, Zhang J, McEachern J, Field H, Daszak P, Eaton BT, Zhang S, Wang LF.** 2005. Bats are natural reservoirs of SARS-like coronaviruses. Science **310:**676–679. http://dx.doi.org/10.1126/science.1118391.
10. **Poon LL, Chu DK, Chan KH, Wong OK, Ellis TM, Leung YH, Lau SK, Woo PC, Suen KY, Yuen KY, Guan Y, Peiris JS.** 2005. Identification of a novel coronavirus in bats. J. Virol. **79:**2001–2009. http://dx.doi.org/10.1128/JVI.79.4.2001-2009.2005.
11. **Vijaykrishna D, Smith GJ, Zhang JX, Peiris JS, Chen H, Guan Y.** 2007. Evolutionary insights into the ecology of coronaviruses. J. Virol. **81:**4012–4020. http://dx.doi.org/10.1128/JVI.02605-06.
12. **Ge XY, Li JL, Yang XL, Chmura AA, Zhu G, Epstein JH, Mazet JK, Hu B, Zhang W, Peng C, Zhang YJ, Luo CM, Tan B, Wang N, Zhu Y, Crameri G, Zhang SY, Wang LF, Daszak P, Shi ZL.** 2013. Isolation and characterization of a bat SARS-like coronavirus that uses the ACE2 receptor. Nature **503:**535–538. http://dx.doi.org/10.1038/nature12711.
13. **Huynh J, Li S, Yount B, Smith A, Sturges L, Olsen JC, Nagel J, Johnson JB, Agnihothram S, Gates JE, Frieman MB, Baric RS, Donaldson EF.** 2012. Evidence supporting a zoonotic origin of human coronavirus strain NL63. J. Virol. **86:**12816–12825. http://dx.doi.org/10.1128/JVI.00906-12.
14. **Du L, He Y, Zhou Y, Liu S, Zheng BJ, Jiang S.** 2009. The spike protein of SARS-CoV—a target for vaccine and therapeutic development. Nat. Rev. Microbiol. **7:**226–236. http://dx.doi.org/10.1038/nrmicro2090.
15. **Berry JD, Hay K, Rini JM, Yu M, Wang L, Plummer FA, Corbett CR, Andonov A.** 2010. Neutralizing epitopes of the SARS-CoV S-protein cluster independent of repertoire, antigen structure or mAb technology. MAbs **2:**53–66. http://dx.doi.org/10.4161/mabs.2.1.10788.
16. **Coughlin M, Lou G, Martinez O, Masterman SK, Olsen OA, Moksa AA, Farzan M, Babcook JS, Prabhakar BS.** 2007. Generation and characterization of human monoclonal neutralizing antibodies with distinct binding and sequence features against SARS coronavirus using XenoMouse. Virology **361:**93–102. http://dx.doi.org/10.1016/j.virol.2006.09.029.
17. **Coughlin MM, Babcook J, Prabhakar BS.** 2009. Human monoclonal antibodies to SARS-coronavirus inhibit infection by different mechanisms. Virology **394:**39–46. http://dx.doi.org/10.1016/j.virol.2009.07.028.
18. **Greenough TC, Babcock GJ, Roberts A, Hernandez HJ, Thomas WD, Jr, Coccia JA, Graziano RF, Srinivasan M, Lowy I, Finberg RW, Subbarao K, Vogel L, Somasundaran M, Luzuriaga K, Sullivan JL, Ambrosino DM.** 2005. Development and characterization of a severe acute respiratory syndrome-associated coronavirus-neutralizing human monoclonal antibody that provides effective immunoprophylaxis in mice. J. Infect. Dis. **191:**507–514. http://dx.doi.org/10.1086/427242.
19. **Lai SC, Chong PC, Yeh CT, Liu LS, Jan JT, Chi HY, Liu HW, Chen A, Wang YC.** 2005. Characterization of neutralizing monoclonal antibodies recognizing a 15-residues epitope on the spike protein HR2 region of severe acute respiratory syndrome coronavirus (SARS-CoV). J. Biomed. Sci. **12:**711–727. http://dx.doi.org/10.1007/s11373-005-9004-3.
20. **Lip KM, Shen S, Yang X, Keng CT, Zhang A, Oh HL, Li ZH, Hwang LA, Chou CF, Fielding BC, Tan TH, Mayrhofer J, Falkner FG, Fu J, Lim SG, Hong W, Tan YJ.** 2006. Monoclonal antibodies targeting the HR2 domain and the region immediately upstream of the HR2 of the S protein neutralize in vitro infection of severe acute respiratory syndrome coronavirus. J. Virol. **80:**941–950. http://dx.doi.org/10.1128/JVI.80.2.941-950.2006.
21. **Prabakaran P, Gan J, Feng Y, Zhu Z, Choudhry V, Xiao X, Ji X, Dimitrov DS.** 2006. Structure of severe acute respiratory syndrome coronavirus receptor-binding domain complexed with neutralizing antibody. J. Biol. Chem. **281:**15829–15836. http://dx.doi.org/10.1074/jbc.M600697200.
22. **Sui J, Li W, Murakami A, Tamin A, Matthews LJ, Wong SK, Moore MJ, Tallarico AS, Olurinde M, Choe H, Anderson LJ, Bellini WJ, Farzan M, Marasco WA.** 2004. Potent neutralization of severe acute respiratory syndrome (SARS) coronavirus by a human mAb to S1 protein that blocks receptor association. Proc. Natl. Acad. Sci. U. S. A. **101:**2536–2541. http://dx.doi.org/10.1073/pnas.0307140101.
23. **ter Meulen J, Bakker AB, van den Brink EN, Weverling GJ, Martina BE, Haagmans BL, Kuiken T, de Kruif J, Preiser W, Spaan W, Gelderblom HR, Goudsmit J, Osterhaus AD.** 2004. Human monoclonal antibody as prophylaxis for SARS coronavirus infection in ferrets. Lancet **363:**2139–2141. http://dx.doi.org/10.1016/S0140-6736(04)16506-9.
24. **Traggiai E, Becker S, Subbarao K, Kolesnikova L, Uematsu Y, Gismondo MR, Murphy BR, Rappuoli R, Lanzavecchia A.** 2004. An efficient method to make human monoclonal antibodies from memory B cells: potent neutralization of SARS coronavirus. Nat. Med. **10:**871–875. http://dx.doi.org/10.1038/nm1080.
25. **Wang S, Chou TH, Sakhatskyy PV, Huang S, Lawrence JM, Cao H, Huang X, Lu S.** 2005. Identification of two neutralizing regions on the severe acute respiratory syndrome coronavirus spike glycoprotein produced from the mammalian expression system. J. Virol. **79:**1906–1910. http://dx.doi.org/10.1128/JVI.79.3.1906-1910.2005.
26. **Zhang H, Wang G, Li J, Nie Y, Shi X, Lian G, Wang W, Yin X, Zhao Y, Qu X, Ding M, Deng H.** 2004. Identification of an antigenic determinant on the S2 domain of the severe acute respiratory syndrome coronavirus spike glycoprotein capable of inducing neutralizing antibodies. J. Virol. **78:**6938–6945. http://dx.doi.org/10.1128/JVI.78.13.6938-6945.2004.
27. **Zhu Z, Chakraborti S, He Y, Roberts A, Sheahan T, Xiao X, Hensley LE, Prabakaran P, Rockx B, Sidorov IA, Corti D, Vogel L, Feng Y, Kim JO, Wang LF, Baric R, Lanzavecchia A, Curtis KM, Nabel GJ, Subbarao K, Jiang S, Dimitrov DS.** 2007. Potent cross-reactive neutralization of SARS coronavirus isolates by human monoclonal antibodies. Proc. Natl. Acad. Sci. U. S. A. **104:**12123–12128. http://dx.doi.org/10.1073/pnas.0701000104.
28. **van den Brink EN, Ter Meulen J, Cox F, Jongeneelen MA, Thijsse A, Throsby M, Marissen WE, Rood PM, Bakker AB, Gelderblom HR, Martina BE, Osterhaus AD, Preiser W, Doerr HW, de Kruif J, Goudsmit J.** 2005. Molecular and biological characterization of human monoclonal antibodies binding to the spike and nucleocapsid proteins of severe acute respiratory syndrome coronavirus. J. Virol. **79:**1635–1644. http://dx.doi.org/10.1128/JVI.79.3.1635-1644.2005.
29. **Cao Z, Liu L, Du L, Zhang C, Jiang S, Li T, He Y.** 2010. Potent and persistent antibody responses against the receptor-binding domain of SARS-CoV spike protein in recovered patients. Virol. J. **7:**299. http://dx.doi.org/10.1186/1743-422X-7-299.
30. **He Y, Zhu Q, Liu S, Zhou Y, Yang B, Li J, Jiang S.** 2005. Identification of a critical neutralization determinant of severe acute respiratory syndrome (SARS)-associated coronavirus: importance for designing SARS vaccines. Virology **334:**74–82. http://dx.doi.org/10.1016/j.virol.2005.01.034.
31. **Lu L, Manopo I, Leung BP, Chng HH, Ling AE, Chee LL, Ooi EE, Chan SW, Kwang J.** 2004. Immunological characterization of the spike protein of the severe acute respiratory syndrome coronavirus. J. Clin. Microbiol. **42:**1570–1576. http://dx.doi.org/10.1128/JCM.42.4.1570-1576.2004.
32. **Zakhartchouk AN, Sharon C, Satkunarajah M, Auperin T, Viswanathan S, Mutwiri G, Petric M, See RH, Brunham RC, Finlay BB, Cameron C, Kelvin DJ, Cochrane A, Rini JM, Babiuk LA.** 2007. Immunogenicity of a receptor-binding domain of SARS coronavirus spike protein in mice: implications for a subunit vaccine. Vaccine **25:**136–143. http://dx.doi.org/10.1016/j.vaccine.2006.06.084.
33. **Zhong X, Yang H, Guo ZF, Sin WY, Chen W, Xu J, Fu L, Wu J, Mak CK, Cheng CS, Yang Y, Cao S, Wong TY, Lai ST, Xie Y, Guo Z.** 2005. B-cell responses in patients who have recovered from severe acute respiratory syndrome target a dominant site in the S2 domain of the surface spike glycoprotein. J. Virol. **79:**3401–3408. http://dx.doi.org/10.1128/JVI.79.6.3401-3408.2005.
34. **Rockx B, Corti D, Donaldson E, Sheahan T, Stadler K, Lanzavecchia A, Baric R.** 2008. Structural basis for potent cross-neutralizing human monoclonal antibody protection against lethal human and zoonotic SARS-CoV challenge. J. Virol. **82:**3220–3235. http://dx.doi.org/10.1128/JVI.02377-07.
35. **Rockx B, Donaldson E, Frieman M, Sheahan T, Corti D, Lanzavecchia A, Baric RS.** 2010. Escape from human monoclonal antibody neutralization affects in vitro and in vivo fitness of severe acute respiratory syndrome coronavirus. J. Infect. Dis. **201:**946–955. http://dx.doi.org/10.1086/651022.
36. **Hwang WC, Lin Y, Santelli E, Sui J, Jaroszewski L, Stec B, Farzan M, Marasco WA, Liddington RC.** 2006. Structural basis of neutralization by a human anti-severe acute respiratory syndrome spike protein antibody, 80R. J. Biol. Chem. **281:**34610–34616. http://dx.doi.org/10.1074/jbc.M603275200.
37. **Sui J, Li W, Roberts A, Matthews LJ, Murakami A, Vogel L, Wong SK, Subbarao K, Farzan M, Marasco WA.** 2005. Evaluation of human monoclonal antibody 80R for immunoprophylaxis of severe acute respiratory syndrome by an animal study, epitope mapping, and analysis of spike variants. J. Virol. **79:**5900–5906. http://dx.doi.org/10.1128/JVI.79.10.5900-5906.2005.
38. **Sui J, Aird DR, Tamin A, Murakami A, Yan M, Yammanuru A, Jing H, Kan B, Liu X, Zhu Q, Yuan QA, Adams GP, Bellini WJ, Xu J, Anderson LJ, Marasco WA.** 2008. Broadening of neutralization activity to directly block a

dominant antibody-driven SARS-coronavirus evolution pathway. PLoS Pathog. **4:**e1000197. http://dx.doi.org/10.1371/journal.ppat.1000197.
39. **Sheahan T, Whitmore A, Long K, Ferris M, Rockx B, Funkhouser W, Donaldson E, Gralinski L, Collier M, Heise M, Davis N, Johnston R, Baric RS.** 2011. Successful vaccination strategies that protect aged mice from lethal challenge from influenza virus and heterologous severe acute respiratory syndrome coronavirus. J. Virol. **85:**217–230. http://dx.doi.org/10.1128/JVI.01805-10.
40. **Yount B, Curtis KM, Fritz EA, Hensley LE, Jahrling PB, Prentice E, Denison MR, Geisbert TW, Baric RS.** 2003. Reverse genetics with a full-length infectious cDNA of severe acute respiratory syndrome coronavirus. Proc. Natl. Acad. Sci. U. S. A. **100:**12995–13000. http://dx.doi.org/10.1073/pnas.1735582100.
41. **Rockx B, Corti D, Donaldson E, Sheahan T, Stadler K, Lanzavecchia A, Baric R.** 2008. Structural basis for potent cross-neutralizing human monoclonal antibody protection against lethal human and zoonotic severe acute respiratory syndrome coronavirus challenge. J. Virol. **82:**3220–3235. http://dx.doi.org/10.1128/JVI.02377-07.
42. **Rockx B, Sheahan T, Donaldson E, Harkema J, Sims A, Heise M, Pickles R, Cameron M, Kelvin D, Baric R.** 2007. Synthetic reconstruction of zoonotic and early human severe acute respiratory syndrome coronavirus isolates that produce fatal disease in aged mice. J. Virol. **81:**7410–7423. http://dx.doi.org/10.1128/JVI.00505-07.
43. **Harrison JL, Williams SC, Winter G, Nissim A.** 1996. Screening of phage antibody libraries. Methods Enzymol. **267:**83–109. http://dx.doi.org/10.1016/S0076-6879(96)67007-4.
44. **Reff ME,Carner K, Chambers KS, Chinn PC, Leonard JE, Raab R, Newman RA, Hanna N, Anderson DR.** 1994. Depletion of B cells in vivo by a chimeric mouse human monoclonal antibody to CD20. Blood **83:**435–445.
45. **Yang ZY, Huang Y, Ganesh L, Leung K, Kong WP, Schwartz O, Subbarao K, Nabel GJ.** 2004. pH-dependent entry of severe acute respiratory syndrome coronavirus is mediated by the spike glycoprotein and enhanced by dendritic cell transfer through DC-SIGN. J. Virol. **78:**5642–5650. http://dx.doi.org/10.1128/JVI.78.11.5642-5650.2004.
46. **Li W, Moore MJ, Vasilieva N, Sui J, Wong SK, Berne MA, Somasundaran M, Sullivan JL, Luzuriaga K, Greenough TC, Choe H, Farzan M.** 2003. Angiotensin-converting enzyme 2 is a functional receptor for the SARS coronavirus. Nature **426:**450–454. http://dx.doi.org/10.1038/nature02145.
47. **Wong SK, Li W, Moore MJ, Choe H, Farzan M.** 2004. A 193-amino acid fragment of the SARS coronavirus S protein efficiently binds angiotensin-converting enzyme 2. J. Biol. Chem. **279:**3197–3201. http://dx.doi.org/10.1074/jbc.C300520200.
48. **Li F, Li W, Farzan M, Harrison SC.** 2005. Structure of SARS coronavirus spike receptor-binding domain complexed with receptor. Science **309:**1864–1868. http://dx.doi.org/10.1126/science.1116480.
49. **Sui J, Hwang WC, Perez S, Wei G, Aird D, Chen LM, Santelli E, Stec B, Cadwell G, Ali M, Wan H, Murakami A, Yammanuru A, Han T, Cox NJ, Bankston LA, Donis RO, Liddington RC, Marasco WA.** 2009. Structural and functional bases for broad-spectrum neutralization of avian and human influenza A viruses. Nat. Struct. Mol. Biol. **16:**265–273. http://dx.doi.org/10.1038/nsmb.1566.
50. **Frieman M, Yount B, Agnihothram S, Page C, Donaldson E, Roberts A, Vogel L, Woodruff B, Scorpio D, Subbarao K, Baric RS.** 2012. Molecular determinants of severe acute respiratory syndrome coronavirus pathogenesis and virulence in young and aged mouse models of human disease. J. Virol. **86:**884–897. http://dx.doi.org/10.1128/JVI.05957-11.
51. **Li W, Greenough TC, Moore MJ, Vasilieva N, Somasundaran M, Sullivan JL, Farzan M, Choe H.** 2004. Efficient replication of severe acute respiratory syndrome coronavirus in mouse cells is limited by murine angiotensin-converting enzyme 2. J. Virol. **78:**11429–11433. http://dx.doi.org/10.1128/JVI.78.20.11429-11433.2004.
52. **Roberts A, Deming D, Paddock CD, Cheng A, Yount B, Vogel L, Herman BD, Sheahan T, Heise M, Genrich GL, Zaki SR, Baric R, Subbarao K.** 2007. A mouse-adapted SARS-coronavirus causes disease and mortality in BALB/c mice. PLoS Pathog. **3:**e5. http://dx.doi.org/10.1371/journal.ppat.0030005.
53. **Li W, Zhang C, Sui J, Kuhn JH, Moore MJ, Luo S, Wong SK, Huang IC, Xu K, Vasilieva N, Murakami A, He Y, Marasco WA, Guan Y, Choe H, Farzan M.** 2005. Receptor and viral determinants of SARS-coronavirus adaptation to human ACE2. EMBO J. **24:**1634–1643. http://dx.doi.org/10.1038/sj.emboj.7600640.
54. **Rani M, Bolles M, Donaldson EF, Van Blarcom T, Baric R, Iverson B, Georgiou G.** 2012. Increased antibody affinity confers broad in vitro protection against escape mutants of severe acute respiratory syndrome coronavirus. J. Virol. **86:**9113–9121. http://dx.doi.org/10.1128/JVI.00233-12.
55. **Lai MM, Cavanagh D.** 1997. The molecular biology of coronaviruses. Adv. Virus Res. **48:**1–100.
56. **Corti D, Lanzavecchia A.** 2013. Broadly neutralizing antiviral antibodies. Annu. Rev. Immunol. **31:**705–742. http://dx.doi.org/10.1146/annurev-immunol-032712-095916.